Co-Designed Quasi-Circulator and Bandpass Filter

Andrea Ashley#1 and Dimitra Psychogiou#2

*Department of Electrical, Computer, and Energy Engineering, University of Colorado Boulder, Boulder, CO, USA {\textsupering Ashley, \textsupering Dimitra.Psychogiou} @colorado.edu

Abstract—This paper focuses on RF co-designed front-end components that simultaneously exhibit the function of a quasicirculator (QC) and a bandpass filter (BPF). They are based on transistor-based non-reciprocal stages that are effectively combined with a Wilkinson divider and/or passive resonators. RF front-end miniaturization is achieved through: i) a magnetic-free design method that exploits the inherent non-reciprocal properties of transistors and ii) the realization of an RF component with colocated signal processing actions. For proof-of-concept validation purposes, two QC/BPF prototypes were designed, manufactured and measured at 2.4 GHz. The first prototype exhibited a singlepole BPF response with minimum in-band insertion loss (IL) of 0.9 dB, 3-dB FBW of 18.9% and maximum isolation (IS) of 21 dB, 16.9 dB and 46 dB for respectively RF signal transmission between ports 1 and 2, 1 and 3 and 2 and 3. The second prototype exhibited a two-pole BPF response with minimum in-band IL of 0.5 dB, 3dB FBW of 14.6%, and maximum IS of 21.3 dB, 20.3, and 47.4 dB for respectively RF signal transmission between ports 1 and 2, 1 and 3 and 2 and 3.

Keywords — Bandpass filter, circulator, isolator, non-reciprocal filter, quasi-circulator, RF co-design.

I. INTRODUCTION

Full-duplex spectrum access has been long discussed as one of the most prominent solutions for increasing spectral efficiency. However, the practical development of RF transceivers able to support this operation has been hindered by the lack of compact RF hardware to isolate the transmit (Tx) from the receive (Rx) mode of operation. Conventional approaches using ferrite-based non-reciprocal components (e.g., circulators, isolators) [1]-[2] or simultaneous transmit and receive (STAR) antennas [3] are bulky (commercial circulators can be on the order for $0.54\lambda \times 0.55\lambda \times 0.24\lambda$ [4]) and incompatible with IC integration. Whereas the size of commercially-available ferrite-based circulators is limited by the need for external magnetic biasing, [1]-[2], STAR-based antenna interfaces are restricted by the use of widely-spaced antenna elements [3].

RF front-end miniaturization techniques of full-duplex systems are mostly focused on magnetless RF circulator-concepts using self-biased magnetic materials and transistor-based integration schemes. The self-biased circulator schemes use magnetic materials with high magnetic anisotropy (e.g., hexaferrites [5] and magnetic nanowires [6]), however most of these materials are in their infancy and result in prohibitively large insertion loss (IL) of about 8 dB, [6]. Transistor-based circulator/quasi-circulator (QC) approaches exploit the inherent non-reciprocal properties of transistors and are better suited for IC/low-profile integration. Examples of these concepts include:

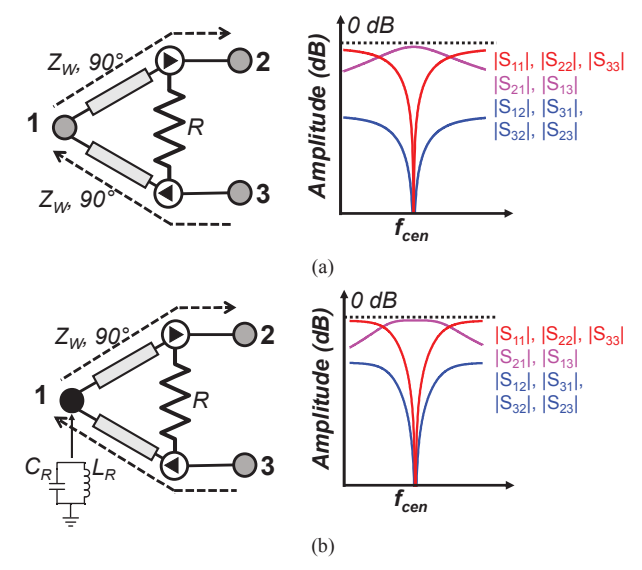


Fig. 1. RF co-designed QC/BPF based on non-reciprocal transistor-based resonant stages (white circle), reciprocal passive resonators (black circles) and a Wilkinson power divider (shaped by two 90°-long TLs at f_{cen} and one resistor R). The grey rectangles represent 90°-long TLs at f_{cen} and the grey circles denote input/output ports. Dashed lines indicate how the RF signal flows. (a) Circuit-schematic and conceptual power transmission, reflection, and isolation response of a QC/BPF shaped by one transistor-based stage (one-pole response). (b) Circuit-schematic and conceptual power transmission, reflection, and isolation response of a QC/BPF shaped by one transistor-based stage and one passive resonator for increased selectivity (two-pole response) in the forward RF signal paths.

i) circulators using transistors and transmission-line (TL) feedback networks [7], and ii) QC architectures using distributed-amplifier configurations or transistor-based feedback networks combined with Lange couplers [8] and Wilkinson dividers [9]. However, they exhibit high IL (3.5-5.7dB in [8]-[9]) and moderate levels of isolation (12-22 dB) [8].

To further reduce the RF front-end size, RF co-design methods of front-end components with collocated RF signal processing capabilities are currently being explored. Notable demonstrations of RF co-designed components include power dividers with bandpass filter (BPF) capabilities [10] and frequency-selective single- and multi-band matching networks [11]. This paper explores for the first time a new class of RF co-designed front-end components that simultaneously perform the function of a BPF and a QC. They are based on transistor-based non-reciprocal stages that are effectively combined with a Wilkinson divider and/or passive resonators. RF front-end

miniaturization is achieved through: i) magnetic-free design methods that exploit the non-reciprocal properties of transistors and ii) the realization of an RF component with co-located signal processing actions, namely a BPF and a QC.

The content of this paper is organized as follows. Section II, presents the theoretical foundations of the RF co-designed QC/BPF. The experimental validation of this concept is reported in Section III. Lastly, the major contributions of this work are summarized in Section IV.

II. THEORETICAL FOUNDATIONS

A. Quasi-Circulator/Bandpass Filter Concept

The details of the RF co-designed QC/BPF concept are shown in Fig. 1. It is based on fully-directional transistor-based resonant stages (white circles) that are effectively combined with a Wilkinson divider to functionalize a frequency-selective QC. The Tx/Rx separation is performed by connecting two reversely-oriented isolation stages at ports 2 and 3 of the Wilkinson divider as shown in Figs. 1(a), (b). Frequency selectivity is achieved by: i) designing the isolation stages to exhibit a non-reciprocal resonance, as shown in the circuit schematic and its power transmission, isolation and reflection response in Fig. 2, and ii) by incorporating reciprocal resonators at port 1 of the Wilkinson divider. In particular, the circuit schematic in Fig. 1(a)—shaped by one non-reciprocal resonant stage and a Wilkinson divider—allows for a bandpass one-poletype response in the directions of propagation (e.g., from port 1 to 2 or from port 3 to 1) and full signal cancellation in the remaining ones. The frequency-selectivity of the QC can be increased by adding a reciprocal resonator at port 1 of the Wilkinson divider as shown in Fig. 1(b).

B. Non-Reciprocal Resonator Design

The circuit schematic and power transmission, reflection and isolation responses of the non-reciprocal resonant stage are respectively shown in Figs. 2(a) and (b). It is based on two inparallel cascaded sections that are shaped by i) a TL section and ii) a transistor-based path, [12]. The transistor-based path, is shaped by: i) four resistors (R_{GS} , R_{GP} , R_{DS} , and R_{DP}) whose values are appropriately selected to obtain good match, isolation, and enhanced power transmission (i.e., gain) at the designed center frequency f_{cen} , and ii) a pHEMT transistor in common-source configuration. The resonator design starts by defining the operational characteristics of the transistor-based stages for the desired gain and matching levels at the direction of propagation. It is then completed by selecting the TL-based parameters (Z_T and θ) for: i) a zero-phase resonance in the direction of propagation (e.g., from port 1 to 2) and ii) destructive interference cancellation in direction of isolation (e.g., from port 2 to 1).

To better illustrate the operating and design principles of the non-reciprocal resonant stage, an example case is considered in Figs. 2(b), (c) for a commercially-available pHEMT (SKY65050-372LF) transistor from Skyworks Inc. The transistor is biased at $V_{DD} = 2$ V, $I_{DD} = 2$ 0mA and its resistors are selected as: $R_{GS} = 42.2\Omega$, $R_{GP} = 110.2\Omega$, $R_{DS} = 34.4\Omega$, and $R_{DP} = 56.6\Omega$. In this manner, a gain of 2.5 dB is obtained at the

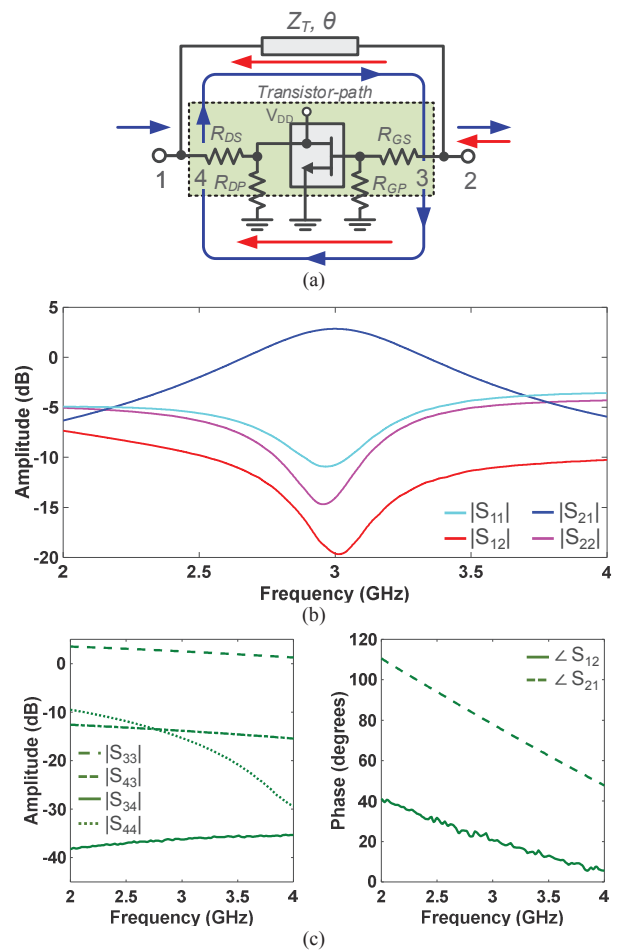


Fig. 2. Non-reciprocal transistor-based resonant stage. (a), (b) Circuit-schematic and its corresponding power transmission, isolation and input-reflection response. (c) Power transmission response of the transistor-based path in terms of amplitude and phase. The illustrated examples were obtained from circuit schematics that comprise transistor-based sections with the following elements: Skyworks SKY65050-372LF pHEMT, R_{GS} = 42.1 Ω , R_{GP} = 110.2 Ω , R_{DS} = 34.4 Ω , R_{DP} = 56.6 Ω , Z_T = 24.2 Ω , θ =86°.

design frequency of interest (3 GHz in this case) as shown in its power transmission/reflection response in Fig. 2(b). Taking into consideration that the phase response of the transistor-based stage is \angle S43=+78° in one direction e.g., from port 3 to 4 and \angle S34=+20° in the other one, if cascaded in parallel with a TL element with Z_T = 24 Ω and θ =86°, it results a in zero-phase resonance at 3 GHz in the direction of propagation and full RF signal cancellation in the reverse one through destructive interference cancellation. This is shown in the S-parameter response of the overall non-reciprocal resonant stage in Fig. 2(b). As shown, it exhibits a transfer function in the direction of propagation with a selectivity similar to the one obtained by a one-pole BPF.

C. QC/BPF Design

Having designed the non-reciprocal resonant stage, the simplest form of a co-designed QC/BPF can be created by connecting two reversely-oriented non-reciprocal resonant

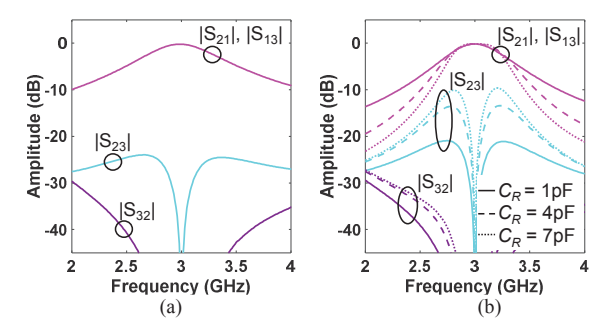


Fig. 3. RF power transmission ($|S_{21}|$, $|S_{13}|$) and isolation ($|S_{23}|$, $|S_{32}|$) response of the QCs/BPFs. (a) S-parameters of the QC/BPF in Fig. 1(a). (b) S-parameters of the QC/BPF in Fig. 1(b) as a function of the capacitance C_R of the passive resonator (designed to resonate at f_{cen}).

stages at the output ports (2,3) of a Wilkinson divider as shown in Fig. 1(a). To better illustrate the operating principles of this device, a first-order QC/BPF was designed with linear circuit-simulations and using as a reference the non-reciprocal resonant stage in Fig. 2. Its response is plotted in Fig. 3(a). As shown, a single-pole BPF response is obtained in the directions of propagation (S_{21}, S_{13}) and maximum signal cancellation in the reversed ones $(S_{23}, S_{32}, S_{12}, \text{ and } S_{31})$.

To increase the passband selectivity and allow for BW control, without significantly altering the footprint of the QC/BPF in Fig. 1(a), a reciprocal resonator—e.g., parallel LC resonator (L_R , C_R)—can be added at port 1 of the single-pole QC as shown in Fig. 1(b). In this manner, a two pole BPF transfer function is obtained in the direction of propagation. In particular, the pole created by the reciprocal resonator (L_R , C_R) is effectively coupled with the pole of the non-reciprocal

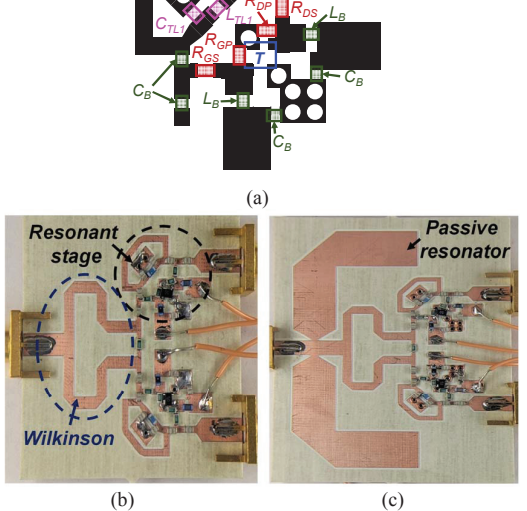


Fig. 4. Manufactured prototypes of the QC/BPFs. (a) Close-up view of the layout of the resonant stage with labeled SMDs: T: SKY65050-372LF, R_{GS} = 38.3 Ω , R_{GP} = 133 Ω , R_{DS} = 12 Ω , R_{DP} = 68.1 Ω , C_{TLI} = 1 pF, L_{TLI} = 2.2 nH, C_B = 3.9 pF and L_B = 120 nH. (b) One-pole QC/BPF using as a basis the circuit-schematic in Fig. 1(a). (c) Two-pole QC/BPF using as a basis the circuit-schematic in Fig. 1(b).

resonant stage due to the presence of Z_W . Specifically, Z_W performs the function of an inter-resonator coupling between the two resonances and results in a power transmission response in the direction of propagation shaped by two poles. Z_W is preset to provide equal power splitting between the paths and can't be altered to control BW. BW controllability, however, can be achieved by altering C_R as shown in the design example in Fig. 3(b). As shown, reciprocal resonators with larger C_R result in narrower BW states and decreased isolation levels in the reverse direction.

III. EXPERIMENTAL VALIDATION

To evaluate the validity of the proposed RF co-designed QC/BPF concept, two prototypes were designed, manufactured, and measured for a center frequency of 2.4 GHz and fractional bandwidth (FBW) of 18.9 and 14.6%, for respectively the one-pole and the two-pole QC. The first prototype is based on the single-pole QC in Fig. 1(a), whereas the second on the two-pole QC in Fig. 1(b). The design was performed with full-wave post-layout electromagnetic simulations in the software package Advanced Design System (ADS) from Keysight using as a reference the measured S-parameters of the Skyworks SKY65050-372LF for $V_{DD} = 2V$, $I_{DD} = 20$ mA. The prototypes were manufactured on a Rogers 4350B substrate with the following characteristics: thickness h=1.52mm, dielectric permittivity ε_r =3.48, and dielectric loss tangent $\tan \delta$ =0.003 and

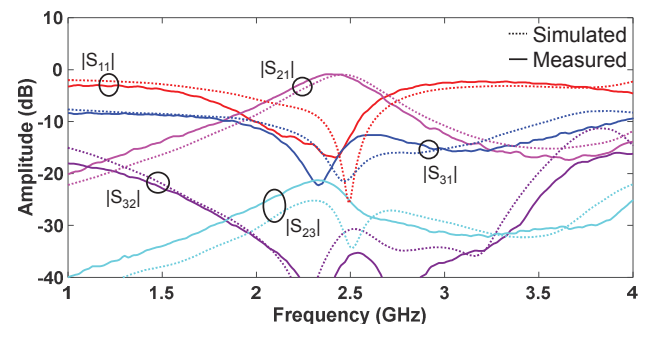


Fig. 5. RF-measured and EM-simulated power transmission and reflection response (forward and reverse directions) of the QC/BPF in Fig. 4(b) that exhibits a single-pole power transmission response in its forward signal paths ($|S_{21}|$, $|S_{13}|$) and full RF signal cancellation in the reversed ones.

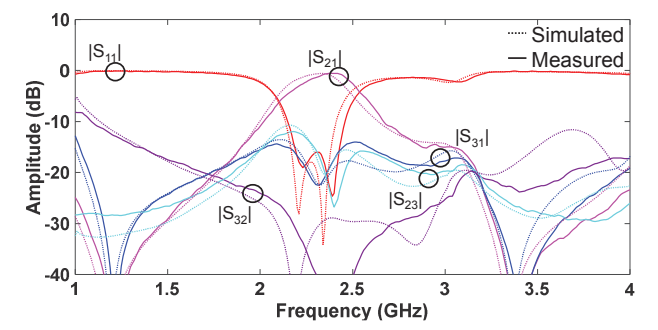


Fig. 6. RF-measured and EM-simulated power transmission and reflection response (forward and reverse directions) of the QC/BPF in Fig. 4(c) that exhibits a two-pole power transmission response in its forward signal paths $(|S_{21}|, |S_{13}|)$ and full RF signal cancellation in the reversed ones.

Table 1. Comparison of the proposed quasi-circulator/BPF with state-of-the-art circulators.

Ref.	Integration Scheme	Frequency (GHz)	Reverse Isolation (dB)	Forward Transmission (dB)	Size (λ x λ)	Filtering Capabilities	P _{DC} (mW)
[2]	Ferrite	9.4	>20	-1	0.81 x 0.81	No	0
[5]	Ferrite, Self-biased	13.65	21	-1.52	0.55 x 0.55	No	0
[6]	Ferrite, Self-biased	11	>35	-8	0.11 x 0.11	No	0
[7]	Microstrip, MESFET	1.8	>35	-2	N/A	No	900
[8]	IC, CMOS	40.5	12 - 22	-3.5	0.13 x 0.13	No	41.8
[9]	IC, CMOS	24	20	-5.7	0.1 x 0.044	No	7.2
This work	Microstrip, pHEMT	2.4	21.3	-0.9	0.31 x 0.3	Yes	132
This work	Microstrip, pHEMT	2.4	26.8	-0.5	0.48 x 0.34	Yes	132

using a mixed integration scheme as shown in Fig. 4. In particular, the Wilkinson divider was implemented using microstrip TLs and the non-reciprocal resonant stage was implemented by both a lumped element and a microstrip TL. A microstrip-type 180° -long resonator is used in the two-pole QC/BPF. It is implemented with two in-parallel connected TLs (Z_0 of $28~\Omega$) due to the need for low characteristic impedance (Z_R =14 Ω) for the realization of the desired FBW-state.

The measured RF performance was characterized in terms of S-parameters with a Keysight 8719A PNA and is shown in Fig. 5 and Fig. 6. A comparison with the EM-simulated S-parameters is also included in these figures which as shown is in a good agreement, successfully validating the proposed RF co-designed QC/BPF concept. While not all of the S-parameters are shown ($|S_{12}|$, $|S_{13}|$, $|S_{22}|$, and $|S_{33}|$ are omitted), they are in a good agreement with the EM simulated ones.

The RF measured characteristics are summarized as follows: single-pole prototype—fcen: 2.4 GHz, minimum in-band IL: 0.9 dB, maximum IS of 21 dB, 16.9 dB, and 46 dB for respectively RF signal transmission between ports 1 and 2, 1 and 3, and 2 and 3; two-pole prototype—center frequency: 2.4 GHz, minimum in-band IL: 0.53 dB, maximum IS of 21.3 dB, 20.3 dB, and 47.4 dB for respectively RF signal transmission between ports 1 and 2, 1 and 3, and 2 and 3. A comparison with state-of-the-art ferrite-based and transistor-based circulators is shown in Table 1. As it can be seen, this is the only RF codesigned non-reciprocal RF component that simultaneously performs the function of a circulator and a BPF. If compared with the rest of the circulator devices, it exhibits smaller physical size and lower IL than the ferrite and self-biased based designs, and is the only transistor-based design with filtering capabilities.

IV. CONCLUSION

This paper reported on the RF design of new types of RF front-end components that simultaneously exhibit the operational characteristics of QC and a BPF. The proposed method is based on transistor-based non-reciprocal stages that are effectively combined with a Wilkinson divider and/or passive resonators and result in one-pole and two-pole power transmission responses in the directions of propagation and full-signal cancellation in the reverse ones. The operating principles of the QC/BPF concept were presented through linear circuit simulation analysis of component using commercially-available pHEMT transistors. For proof-of-concept validation,

two prototypes were built and measured at 2.4 GHz using the commercially available SKY65050-372LF transistor from Skyworks Inc.

ACKNOWLEDGMENT

This work was supported in part by the National Defense Science and Engineering Graduate (NDSEG) Fellowship and the National Science Foundation (NSF) under Grand ECCS-1941315.

REFERENCES

- [1] H. Dong, J. R. Smith and J. L. Young, "A wide-band, high isolation UHF lumped-element ferrite circulator," in *IEEE Microwave and Wireless Components Letters*, vol. 23, no. 6, pp. 294-296, June 2013.
- [2] X. Li, E. Li and G. Guo, "Design of X-band H-plane waveguide Y-junction circulator," The 2012 International Workshop on Microwave and Millimeter Wave Circuits and System Technology, Chengdu, 2012, pp. 1-4.
- [3] M. A. Elmansouri, A. J. Kee and D. S. Filipovic, "Wideband antenna array for simultaneous transmit and receive (STAR) applications," in *IEEE Antennas and Wireless Propagation Letters*, vol. 16, pp. 1277-1280, 2017.
- [4] RF circulators. [Online]. Available: http://www.e-meca. com/circulator-isolator/rf-circulators/cs-4-000
- [5] J. Wang et al., "Self Biased Y-junction circulator at K_u band," in IEEE Microwave and Wireless Components Letters, vol. 21, no. 6, pp. 292-294. June 2011.
- [6] G. Hamoir, L. Piraux and I. Huynen, "Control of microwave circulation using unbiased ferromagnetic nanowires arrays," in IEEE Transactions on Magnetics, vol. 49, no. 7, pp. 4261-4264, July 2013.
- [7] S. W. Y. Mung and W. S. Chan, "Active three-way circulator using transistor feedback network," in *IEEE Microwave and Wireless Components Letters*, vol. 27, no. 5, pp. 476-478, May 2017.
- [8] S. Hung, K. Cheng and Y. Wang, "An ultra-wideband quasi-circulator with distributed amplifiers using 90 nm CMOS technology," in *IEEE Microwave and Wireless Components Letters*, vol. 23, no. 12, pp. 656-658, Dec. 2013.
- [9] J. Chang, J. Kao, Y. Lin and H. Wang, "Design and analysis of 24-GHz active isolator and quasi-circulator," in *IEEE Transactions on Microwave Theory and Techniques*, vol. 63, no. 8, pp. 2638-2649, Aug. 2015.
- [10] R. Loeches-Sánchez, D. Psychogiou, D. Peroulis and R. Gómez-García, "A class of planar multi-band Wilkinson-type power divider with intrinsic filtering functionality," 2015 IEEE Radio and Wireless Symposium (RWS), San Diego.
- [11] R. Gómez-García, D. Psychogiou and D. Peroulis, "Reconfigurable single/multi-band planar impedance transformers with incorporated bandpass filtering functionality," 2016 IEEE MTT-S International Microwave Symposium (IMS), San Francisco, CA, 2016, pp. 1-4.
- [12] A. Ashley and D. Psychogiou, "Non-reciprocal RF-bandpass filters using transistor-based microwave resonators," 2019 49th European Microwave Conference (EuMC), Paris, France, 2019, pp. 603-606.